PROCEEDINGS OF THE CALIFORNIA ACADEMY OF SCIENCES

Series 4, Volume 62, Part 2, No. 16, pp. 399–415, 15 figs., 8 tables August 14, 2015

X-ray Microanalysis and the Chemical Elemental Composition of Gorgonian and Pennatulacean Axial Structures (Anthozoa, Octocorallia)

Jei-Ying Chen and Gary C. Williams

California Academy of Sciences, 55 Music Concourse Drive, San Francisco, California 94118 USA
Email: cchen@calacademy.org; gwilliams@calacademy.org

By comparing the elemental compositions of the axes of five families of octocorals from both calcaxonian gorgonians and sea pens using energy dispersive X-ray microanalysis, the aim of this study is to gain insight relating to the phylogenetic relationships between these two groups of octocorals. The overall results across the specimens examined suggest that both groups of octocorals share similar elemental compositions and, therefore, offer little help in inferring phylogeny among taxa. However, this study also suggests the potential for a novel avenue of research for environmental impact assessments by using X-ray microanalysis to obtain the chemical compositions of the calcaxonian gorgonians and sea pens to evaluate the impact of ambient seawater composition with respect to various trace elements.

KEYWORDS: octocorals, Calcaxonia, gorgonians, sea pens, Pennatulacea, X-ray microanalysis

Few papers have been published on mineral content, mineralization, and elemental composition of the skeletal components of octocorals and of these the three most relevant to this study include Folk (1974), MacIntyre, et al. (2000), and Bayer and MacIntyre (2001).

Grasshoff (1999; Grasshoff and Bargibant 2001) proposed and described the group name Calcaxonia for gorgonian families that share the character of a heavy calcified axis, that is solid throughout, and in which the calcified portion is dominant in comparison to the proteinaceous portion. He included the five families, Ifalukellidae, Chrysogorgiidae, Primnoidae, Ellisellidae, and Isididdidae.

Virtually all octocorals have endoskeletal elements in the form of a consolidated central axis or numerous minute sclerites to support the colonies. Both calcaxonian gorgonians and sea pens have solid central axes and have been hypothesized as sister groups, yet very few studies have been done regarding the axial chemical composition in the calcaxonians and pennatulaceans. Thus one of the central questions is: Do these two groups of octocorals share a similar chemical composition across taxa? We here apply X-ray microanalysis to representative specimens from each family of both calcaxonian gorgonians and pennatulaceans to answer this question.

The overarching goal of this study is to portray the phylogenetic relationships between two groups of octocorals: the calcaxonian gorgonians (sea fans) and the pennatulaceans (sea pens), by examining the morphological characters of the axial skeleton of both groups of octocorals using scanning electron microscopy. The microstructural inspection was undertaken on the transverse cross sections of the bare axes of both groups of octocorals to achieve a detailed understanding and to record the special traits that each taxon revealed. By comparing the characteristics of the specimens inspected between the two groups of octocorals, the preliminary morphological interrelationships can be delineated. This is presumably the first study to compare the two groups using energy dispersive X-ray microanalysis on the axis of octocorals for elemental analysis.

Materials and Methods

Materials.— All of the octocoral specimens used in this study are housed in the Invertebrate Zoology Collection of the California Academy of Sciences. Three gorgonian species, *Ellisella* sp. (family Ellisellidae), *Isis hippuris* (family Isididae), *Plumigorgia hydroides* (family Ifalukellidae), and three sea pen species, *Cavernularia* sp. (family Veretillidae), *Stylatula* sp. (family Virgulariidae) and *Virgularia* sp. (family Virgulariidae), were examined. The detailed collection information for each specimen is given as follows: *Ellisella* sp. (family Ellisellidae); partial colony wet preserved in 75% ethanol; CAS-154877; Palau, Uchelbeluu Reef, Koror, near SW corner 7.00°15.61′N 134.00°31.14′E, 123 m, 1 March 2001; Pat Colin aboard research submersible. *Isis hippuris* (family Isididae); partial colony wet preserved in 75% ethanol; CAS-175045; Taiwan, Taitung County, Green Island, 17 m, 14 July 2007; Cerise Chen. *Plumigorgia hydroides* (family Ifalukellidae); whole colony wet preserved in 95% ethanol; CAS-180888; Philippines, Palawan Province, Calamian Group, Busuanga Island, Magic Reef, 11 m, 24 February 2010; Gary C. Williams. *Virgularia* sp. (family Virgulariidae); Papua New Guinea, *Virgularia* sp. (family Virgulariidae); whole colony wet preserved in 75% ethanol; CAS-099847; Papua New Guinea, Madang Province, Pig [Tab] Island, embayment on W coast of island, "center", 6–15 m, 5 June 1992; Gary C. Williams. *Cavernularia* sp. (family Veretillidae); whole colony wet preserved in 75% ethanol; CAS-103391; Pacific Ocean, South China Sea, Taiwan Strait, Formosa Bank, 40–50 fm; Franz B. Steiner. *Stylatula* sp. (family Virgulariidae); whole colony wet preserved in 75% ethanol; CAS-140902; California, San Francisco Estuary, San Francisco Bay, San Francisco County, between Angel Island and Treasure Island 37.00°50.35′N 122.00°24.35′W, 18 m, 14 August 1973; F. Nichols. Specimens were collected from shallow water via scuba diving, while deeper water specimens were collected by bottom trawling.

SEM sample preparation.— To acquire the bare axes out of the sclerite-impregnated coenenchymal tissue in gorgonians and from the fleshy muscular tissue in pennatulaceans, the axes were first sectioned into fragments using a razor blade or bolt clippers or by bending or twisting the axial skeleton perpendicular to the longitudinal axis until it fractured. Then, the samples were treated with concentrated sodium hypochlorite (NaOCl) for an average of 10–15 minutes depending upon the amount of organic matrix to be removed (Lewis et al. 1992). The bleach-treated axes were then rinsed with distilled water several times, processed with ethanol dehydration (Kim et al. 1992), and then allowed to air dry. The dried axial rods were mounted on aluminum SEM stubs with Electrodag® 502 or Colloidal Graphite, then sputter-coated before imaging using a precision etching coating system (PECS, 682, Gatan Inc, Pleasanton, CA) with carbon; a continuous line of silver paint was also applied along the sides of each axial rod, and to the very bottom (the point where the axis is attached on the stub) to facilitate conductivity.

SEM imaging and X-Ray microanalysis.— The SEM images and X-ray microanalysis were taken on a Zeiss Ultra 55 field emission scanning electron microscope equipped with an Oxford INCA energy dispersive spectrometer (EDS). The Everhart-Thornley detector (SE2) and angle selected backscatter (AsB) detector were used at 25 kV accelerating voltage and 60 μm of aperture size in high beam current condition (to allow effective excitation of X-ray line energy for elements with higher shell values) with 8.5 mm analytical working distance (for the optimum microanalysis performance purpose) under the frame average noise reduction method.

Results

Calculations of Electron Range (R_{KO}) and X-Ray Range (R_X).— The calculation of electron range (R_{KO}) of calcium (the major element found in all samples other than carbon and oxy-

gen) was carried out using the equation of Kanaya and Okayama (1972) to measure the interaction volume, where A is the atomic weight (g/mole), Z is the atomic number, ρ is the density (g/cm^3), E_0 is the beam energy (keV), and R_{KO} is calculated in micrometers with the constant 0.0276 (Goldstein et al. 2003); by inserting the beam energy 25 keV along with calcium's atomic weight 40.08 g/mole, atomic number 20 and density 1.53 g/cm^3 to the equation, the electron range (R_{KO}) of calcium 16.072 μm was acquired.

$$R_{KO}(\mu m) = \frac{0.0276A}{Z^{0.89}\rho} E_0^{1.67}$$

While the X-ray range of calcium was calculated using the X-ray range equation according to Anderson and Hasler (1966) to measure the depth of X-ray production, where R_X has units of micrometers, E is in keV and ρ is in g/cm^3; E_C is the critical ionization or exciting energy, also known as the excitation potential or X-ray absorption edge energy (Goldstein et al. 2003). Again using the values of beam energy 25 keV and calcium's density 1.53 g/cm^3, as well as the critical ionization energy of both $K\alpha$ and Lα as 4.038 keV and 0.349 keV, respectively; the X-ray range for calcium $K\alpha$ was acquired as 8.897 μm, and the X-ray range for calcium $L\alpha$, was acquired as 9.326 μm.

$$R_X(\mu m) = \frac{0.064}{\rho}(E_0^{1.68} - E_C^{1.68})$$

SEM/EDS Results

GORGONIANS

Family Isididae

Isis hippuris

Figures 1A–B, 2A–C.

The bar chart in Figure 2B presents the ten elements identified from the axial skeleton of the gorgonian *Isis hippuris*. Three major elements prominently shown in the chart are carbon (21.9 wt%), oxygen (41.71 wt%) and calcium (31.84 wt%); two minor elements are fluorine (1.90 wt%) and magnesium (2.43 wt%); the five remaining trace elements are barely seen from the chart: sodium (0.29 wt%), aluminum (0.07 wt%), sulfur (0.28 wt%), strontium (0.11 wt%) and the rare earth element (REE) ytterbium (0.19 wt%). The summary EDS results for both spectrum 1 (the horizontal site of interest) and spectrum 2 (the vertical site of interest) are listed in Table 1.

TABLE 1. EDS results of spectrum 1 and 2 for gorgonian *Isis hippuris* axial cross-section surface from Figure 2A. (All results are in weight%)

Elements	C	O	F	Na	Mg	Al	S	Ca	Sr	Yb	Total
Spectrum 1	21.17	41.5	1.97	0.29	2.43	0.07	0.29	31.99	0.12	0.18	100
Spectrum 2	21.2	41.91	1.82	0.3	2.43	0.06	0.28	31.68	0.1	0.2	100
Mean	21.19	41.71	1.9	0.29	2.43	0.07	0.28	31.84	0.11	0.19	100
Std. deviation	0.02	0.29	0.1	0.01	0	0.01	0	0.22	0.01	0.01	
Max.	21.2	41.91	1.97	0.3	2.43	0.07	0.29	31.99	0.12	0.2	
Min.	21.17	41.5	1.82	0.29	2.43	0.06	0.28	31.68	0.1	0.18	

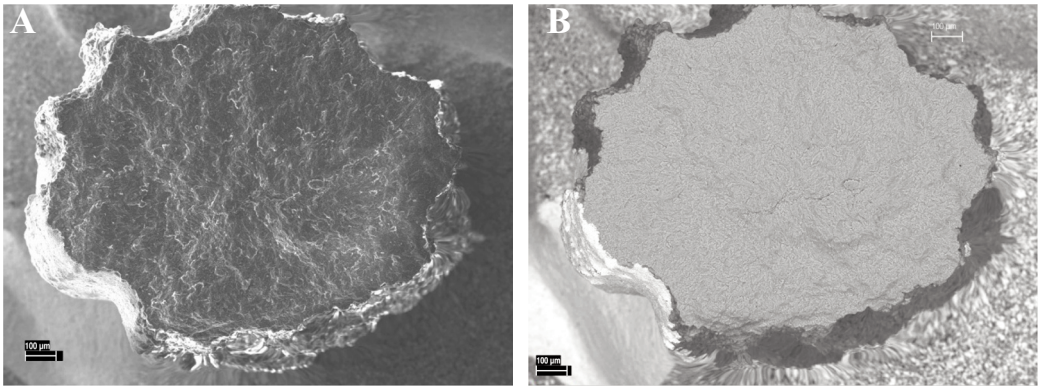

FIGURE 1. Scanning electron microscope (SEM) micrographs of a cross-sectional view of a gorgonian *Isis hippuris* axial skeleton. (A) Secondary electron (SE) image. Scale bar = 100 µm. (B) Back-scattered electron (BSE) image. Scale bar = 100 µm. In both images the charging effect is visible from the lower right corner, where some distortion occurred alongside the axial rod, while no such effect occurred in the silver paint covered area. No significant chemical composition change can be observed from the BSE image due to the lack of contrast across the surface of the axis.

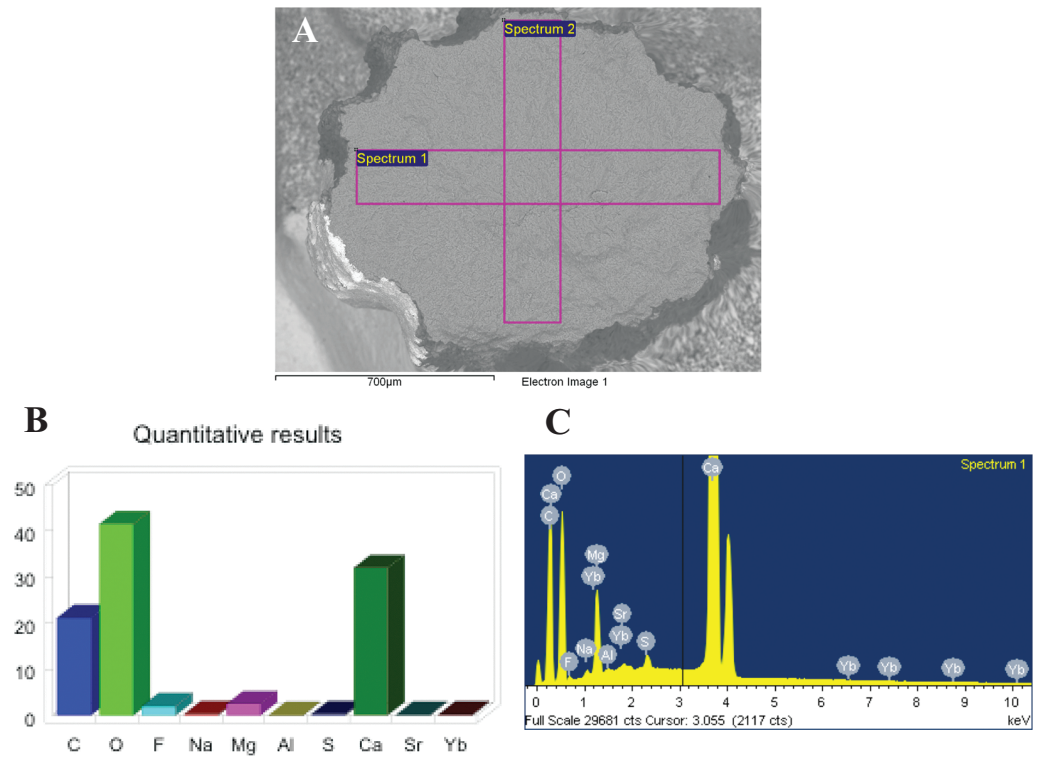

FIGURE 2. Energy dispersive spectrometer (EDS) area scan dataset. (A) EDS site of interest BSE image in a cross-sectional view of a gorgonian *Isis hippuris* axial skeleton acquired by INCA Energy software using the same region as Figure 1, where spectrum 1 was collected across the full span of the maximum horizontal length of the axial surface and spectrum 2 was collected across the full span of the maximum vertical length of the axial surface. Scale bar = 100 µm. (B) Bar chart of the quantitative results from (C) spectrum 1 for reference in that the analytical results of the two sites are fairly similar as presented in Table 1.

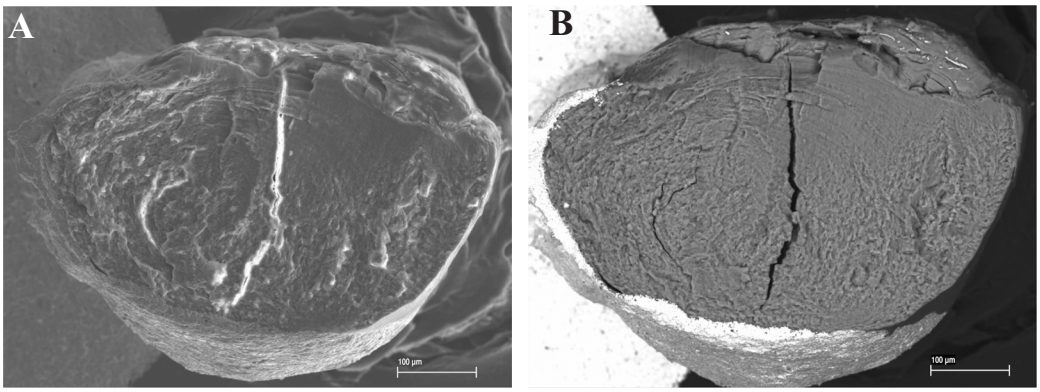

FIGURE 3. Scanning electron microscope (SEM) micrographs of a cross-sectional view of a gorgonian *Plumigorgia hydroides* axial skeleton. (A) Secondary electron (SE) image. The crack appearing in the center of the axis is an artifact caused by the dehydration of the axis (specimen was wet preserved in 95% ethanol); charging was built up inside the crack resulting in the very bright band along the crack region. Scale bar = 100 µm. (B) Back-scattered electron (BSE) image. There is no visible chemical composition change on the surface of the axis except the bright spots on the upper right corner caused by contamination from remnants of razor blade that attached on top of the surface. Scale bar = 100 µm.

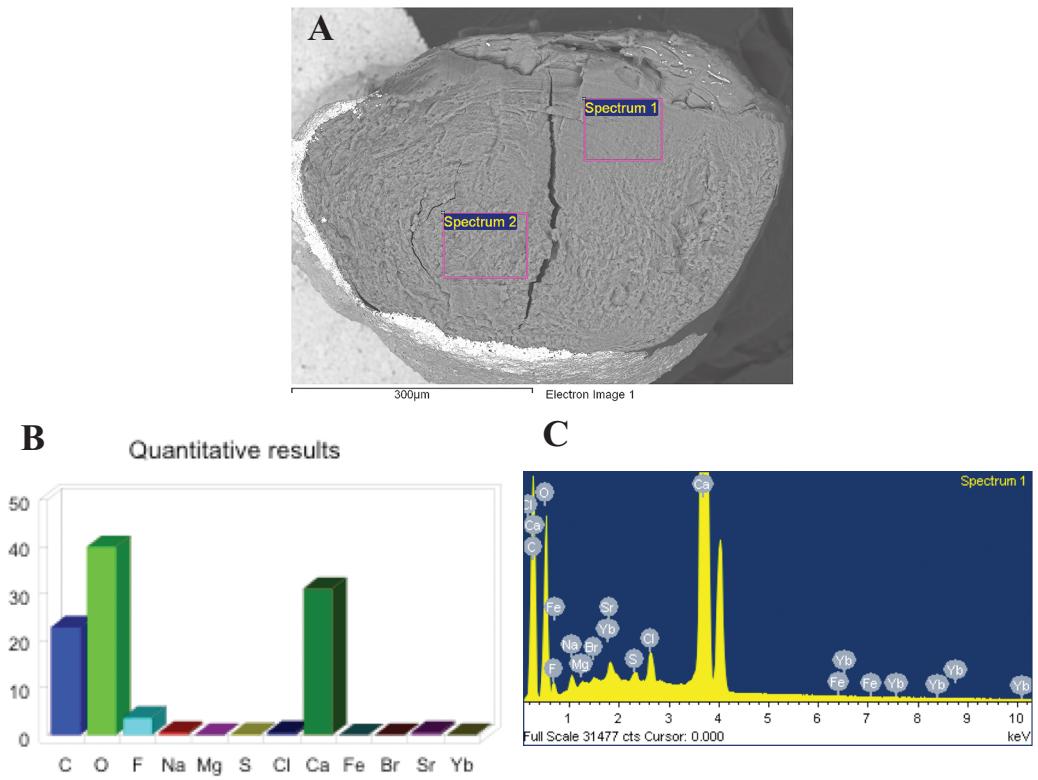

FIGURE 4. Energy dispersive spectrometer (EDS) area scan dataset. (A) EDS site of interest BSE image in a cross-sectional view of a gorgonian *Plumigorgia hydroides* axial skeleton acquired by INCA Energy software using same region as Figure 3, partial area scan was applied due to the visible topographical differences of the surfaces on both sides of the axis, thus only two small areas were selected for EDS analysis. Scale bar = 300 µm. (B) Bar chart of the quantitative results from (C) spectrum 1 for reference in that the analytical results of the two sites are identical as seen in Table 2.

Family Ifalukellidae

Plumigorgia hydroides
Figures 3A–B, 4A–C.

As seen in Figure 4B, there are twelve identified elements, two more than that in *Isis hippuris* in which the major elements present in the axis of *Plumigorgia hydroides* are again carbon (21.93 wt%), oxygen (40.07 wt%) and calcium (32.11 %), with one minor element fluorine found at 3.87 wt%. The remaining trace elements are sodium (0.55 wt%), magnesium (0.07 wt%), sulfur (0.15 wt%), chlorine (0.45 wt%), iron (0.04 wt%), bromine (0.09 wt%), strontium (0.53 wt%) and REE ytterbium (0.14 wt%). The summary EDS results for both spectrum 1 (the right side of the axis) and spectrum 2 (the left side of the axis) are listed in Table 2.

TABLE 2. EDS results of spectrum 1 and 2 for gorgonian *Plumigorgia hydroides* axial cross-section surface from Figure 4A. (All results are in weight%)

Spectrum	C	O	F	Na	Mg	S	Cl	Ca	Fe	Br	Sr	Yb	Total
Spectrum 1	22.92	40.01	3.7	0.55	0.08	0.18	0.62	31.13	0.04	0.1	0.58	0.1	100
Spectrum 2	20.95	40.14	4.04	0.56	0.07	0.11	0.29	33.08	0.03	0.07	0.47	0.18	100
Mean	21.93	40.07	3.87	0.55	0.07	0.15	0.45	32.11	0.04	0.09	0.53	0.14	100
Std. deviation	1.39	0.1	0.24	0.01	0.01	0.05	0.23	1.38	0	0.03	0.07	0.06	
Max.	22.92	40.14	4.04	0.56	0.08	0.18	0.62	33.08	0.04	0.1	0.58	0.18	
Min.	20.95	40.01	3.7	0.55	0.07	0.11	0.29	31.13	0.03	0.07	0.47	0.1	

Family Ellisellidae

***Ellisella* sp.**
Figures 5A–B, 6A–D.

From the linescan BSE image and the element linescan graph (Figure 6A and 6B) a high amount of calcium in the blue line can be seen spread through the horizontal axis surface, with an apparently declining pattern in the central axis region; the same trends can be observed in carbon (in red, 23.75 wt%), oxygen (in orange, 37.69 wt%) and magnesium (in light green, 2.14 wt%), which suggests that the core region of the axis contains lower amounts of the three major elements carbon (23.75 wt%), oxygen (37.69 wt%) and calcium (31.89 wt%), as well as magnesium (2.14 wt%), one of the two minor elements other than fluorine (3.40 wt%). All other trace elements like sodium (0.36 wt%), aluminum (0.05 wt%), sulfur (0.30 wt%), chlorine (0.23 wt%), iron (0.04 wt%), strontium (0.13 wt%) and REE ytterbium (0.14 wt%) have a more evenly distributed pattern with much flatter overall trends along the line. The weight percentage of all twelve identified elements is given in Table 3.

TABLE 3. EDS results of the sum spectrum for the gorgonian *Ellisella* sp. axial cross-section surface from Figure 6A. (All results are in weight%)

Element	C	O	F	Na	Mg	Al	S	Cl	Ca	Fe	Sr	Yb	Total
Sum Spectrum (Weight%)	23.75	37.69	3.4	0.36	22.14	0.05	0.3	0.23	31.89	0.04	0.13	0.01	100

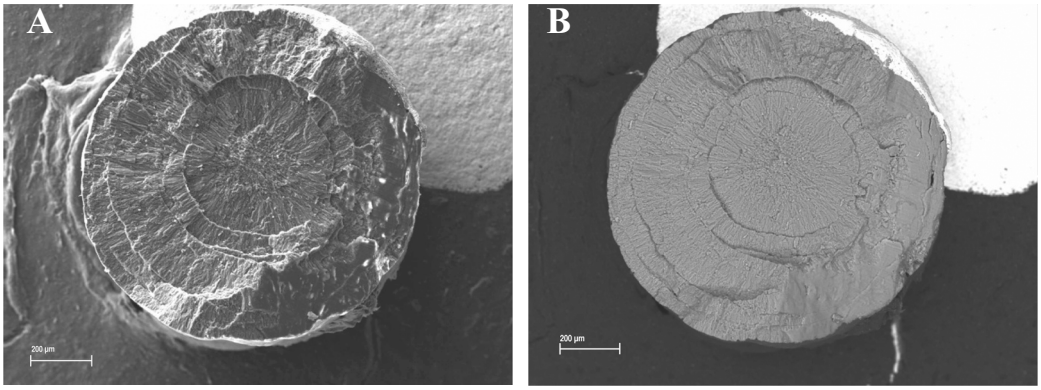

FIGURE 5. Scanning electron microscope (SEM) micrographs of a cross-sectional view of a gorgonian *Ellisella* sp. axial skeleton. (A) Secondary electron (SE) image. The axis of *Ellisella* sp. is featured by the concentric growth rings resembling that in trees, also by the slightly radiating patterns on the surface. These characters are useful for comparative morphology studies on calcaxonian gorgonians and sea pens. Scale bar = 200 µm. (B) Back-scattered electron (BSE) image. The compositional change is minute since again no detectable contrast is observed in the image though the topographical contrast is apparent like that in the SE image. Scale bar = 200 µm.

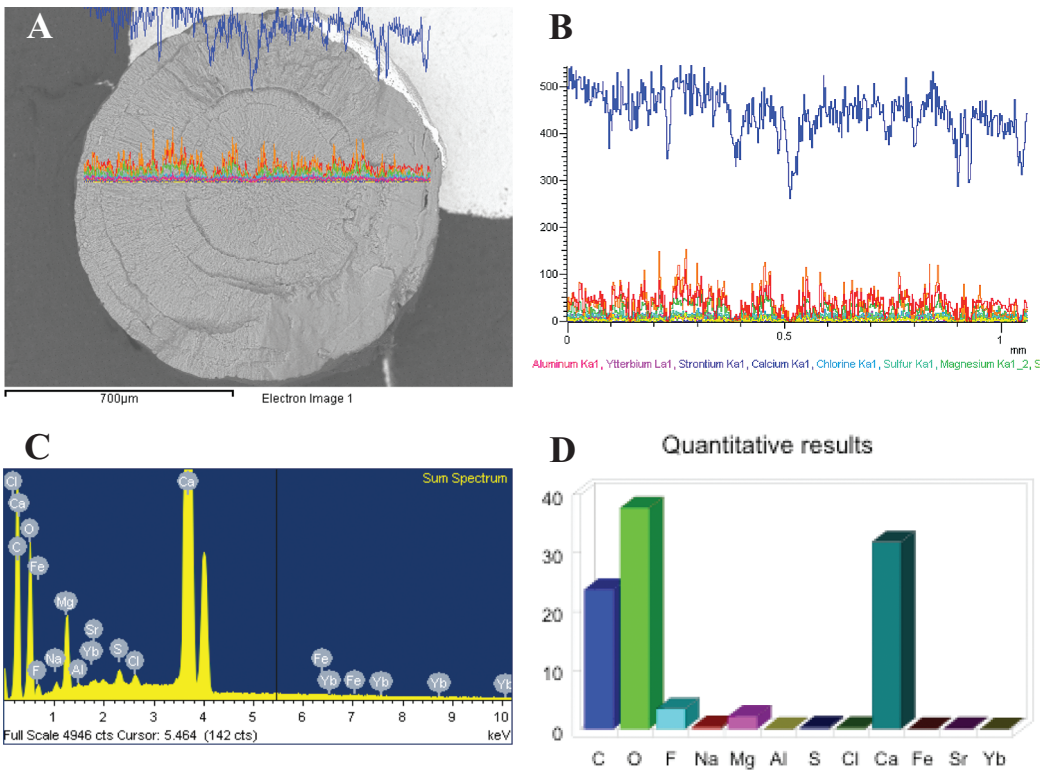

FIGURE 6. Energy dispersive spectrometer (EDS) linescan dataset. (A) EDS linescan site of interest BSE image in a cross-sectional view of a gorgonian *Ellisella* sp. axial skeleton acquired by INCA Energy software using same region as Figure 5, horizontal linescan through the middle of the axis was applied for EDS analysis to examine the distribution of elements along the line. Scale bar = 700 µm. (B) Element linescan result displaying grouped linescans as colored: carbon (red), oxygen (orange), fluorine (yellow), sodium (light green), magnesium (green), aluminum (pink), sulfur (aqua), chlorine (light blue), calcium (blue), strontium (indigo), ytterbium (purple), iron is not shown in the graph. (C) Sum spectrum of the linescan. (D) Bar chart of the quantitative results from the sum spectrum.

Sea Pens

Family Veretillidae

***Cavernularia* sp.**
Figures 7A–B, 8A–D.

In contrast to the linescan patterns of the gorgonian *Ellisella* sp. which has lower values of carbon (in red), oxygen (in orange), calcium (in blue) and magnesium (in light green) in the central core region, the linescan graph Figure 8A showed no significant declination of all four elements on the site of central core region of the sea pen *Cavernularia* sp.; instead, the weight percentage of carbon, oxygen and magnesium are even higher than the other parts of the line section. However, declining patterns of those four elements can still be seen on the site approximately 400 μm away from the left edge of the axial surface, which may be related to the rough surface features shown in Figure 7A that caused the drop of values in the four elements stated above. Besides the three major elements of carbon (17.44 wt%), oxygen (46.43 wt%), calcium (31.35wt%) along with the two minor elements fluorine (1.03 wt%) and magnesium (2.84 wt%), five other trace elements were identified: sodium (0.3 wt%), aluminum (0.06 wt%), sulfur (0.27 wt%), strontium (0.19 wt%) and REE ytterbium (0.11 wt%). All five trace elements and fluorine have flat and steady patterns of line trends compared to that of carbon, oxygen, calcium and magnesium. The weight percentage value of all ten identified elements can be found in Table 4.

Table 4. EDS results of the sum spectrum for sea pen *Cavernularia* sp. axial cross-section surface from Figure 8A. (All results are in weight%)

Spectrum	C	O	F	Na	Mg	Al	S	Ca	Sr	Yb	Total
Sum Spectrum (Weight%)	17.44	46.43	1.03	0.3	2.84	0.06	0.27	31.35	0.19	0.11	100

***Virgularia* sp.**
Figures 9A–B, 10A–D.

Like the observations in the previous specimens, some degree of fluctuations and shift of linescans of carbon (in purple, 20.42 wt%), oxygen (in light green, 44.95 wt%), calcium (in green, 29.35 wt%) and magnesium (in dark green, 2.57 wt%) are found on *Virgularia* sp. as well (Figure 10B); they are mostly found along the central axis region, which may be implied by the BSE image that shows the darker contrast region in the central core of the axis. The fluctuated patterns are consistent among the four elements, thus a clear grouped relationship can be seen when zooming to higher magnification in Fig 10B. The linescan patterns of fluorine (in pink, 1.60 wt%) and the four remaining trace elements sodium (in blue, 0.55 wt%), sulfur (in sky blue, 0.30 wt%), chlorine (in red, 0.07 wt%) and REE ytterbium (in orange, 0.19 wt%) are similar in nature, with an evenly displayed appearance along the linescan section. Table 5 displays the weight percentage value of all nine identified elements.

Table 5. EDS results of the sum spectrum for sea pen *Virgularia* sp. axial cross-section surface from Figure 10A. (All results are in weight%)

Spectrum	C	O	F	Na	Mg	S	Cl	Ca	Yb	Total
Sum Spectrum (Weight%)	20.42	44.95	1.6	0.55	2.57	0.3	0.07	29.35	0.19	100

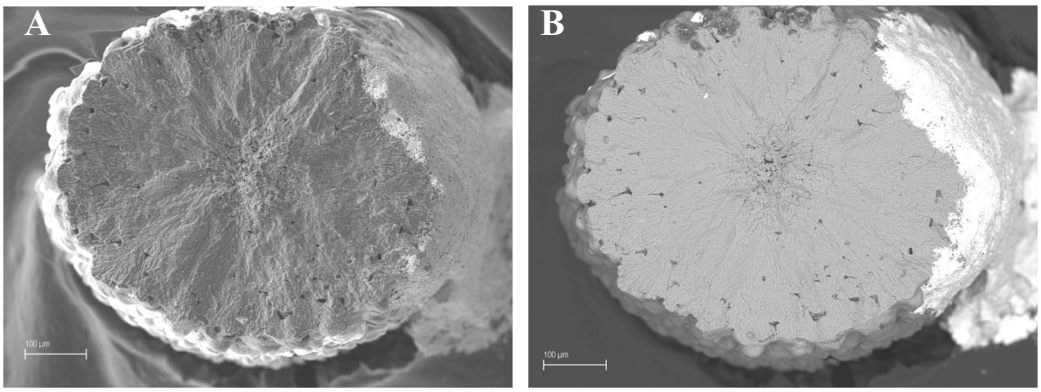

FIGURE 7. Scanning electron microscope (SEM) micrographs of a cross-sectional view of a sea pen *Cavernularia* sp. axial skeleton. (A) Secondary electron (SE) image shows an uneven fracture surface of the axis and multiple comma-like indents around the outer rim of the axial surface known as the imprints of chimney cell extensions according to Ledger and Franc (1978). Scale bar = 100 µm. (B) Back-scattered electron (BSE) image. Same as the previous specimens examined, there are no perceivable compositional changes on the imaging area of axial surface, yet the topographical differences and more chimney cell extensions are clearly shown. Scale bar = 100 µm.

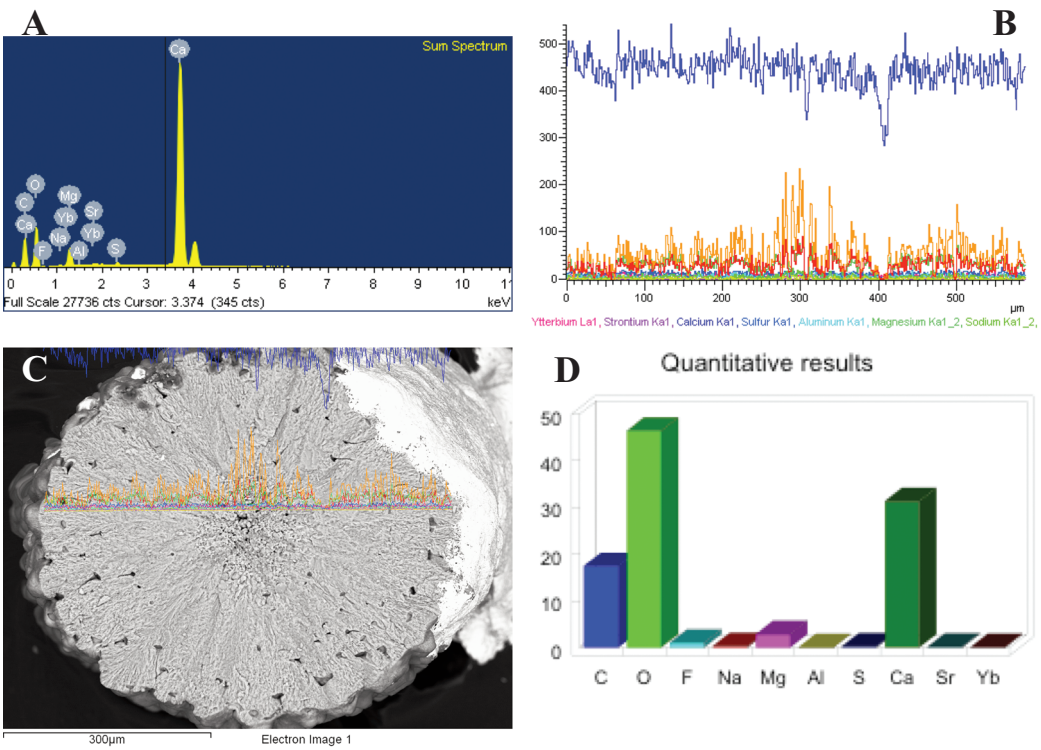

FIGURE 8. Energy dispersive spectrometer (EDS) linescan dataset. (A) EDS linescan site of interest BSE image in a cross-sectional view of a sea pen *Cavernularia* sp. axial skeleton acquired by INCA Energy software using same region as Figure 7, horizontal linescan through the middle of the axis was applied for EDS analysis to examine the distribution of elements along the line. (B) Element linescan result displaying grouped linescans as colored: carbon (red), oxygen (orange), fluorine (yellow), sodium (light green), magnesium (green), aluminum (aqua), sulfur (light blue), calcium (blue), strontium (purple), ytterbium (pink). (C) Sum spectrum of the linescan. Scale bar = 300 µm. (D) Bar chart of the quantitative results from the sum spectrum.

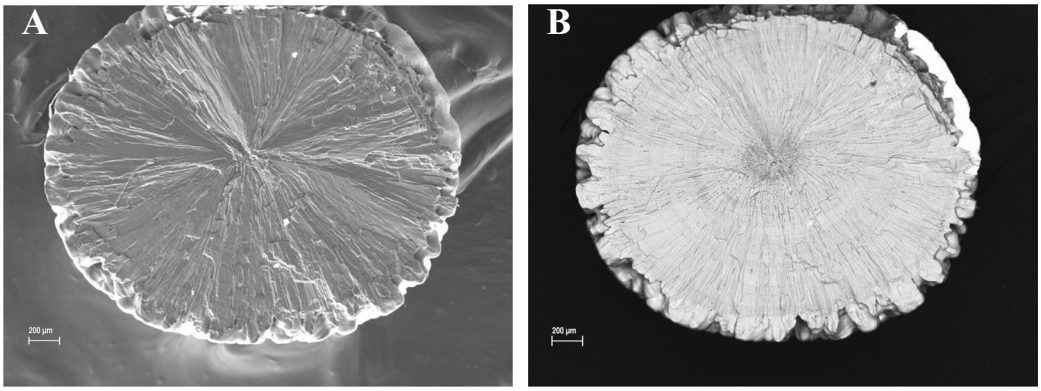

FIGURE 9. Scanning electron microscope (SEM) micrographs of a cross-sectional view of a sea pen *Virgularia* sp. axial skeleton. (A) In this secondary electron (SE) image a great degree of the radiating patterns well-arranged across the whole axial surface can be observed, such character is also used in the morphological phylogenetic studies of the calcaxonian gorgonians and sea pens. Scale bar = 200 µm. (B) Back-scattered electron (BSE) image. There seemed to be some chemical composition contrast appearing darker in the central portion of the axis, though several between-site area scans were performed, yet no differences in chemical composition can be found (data not shown); however, the between-site changes on weight percentage value of some elements can be detected as shown in the next Figure 10B. Scale bar = 200 µm.

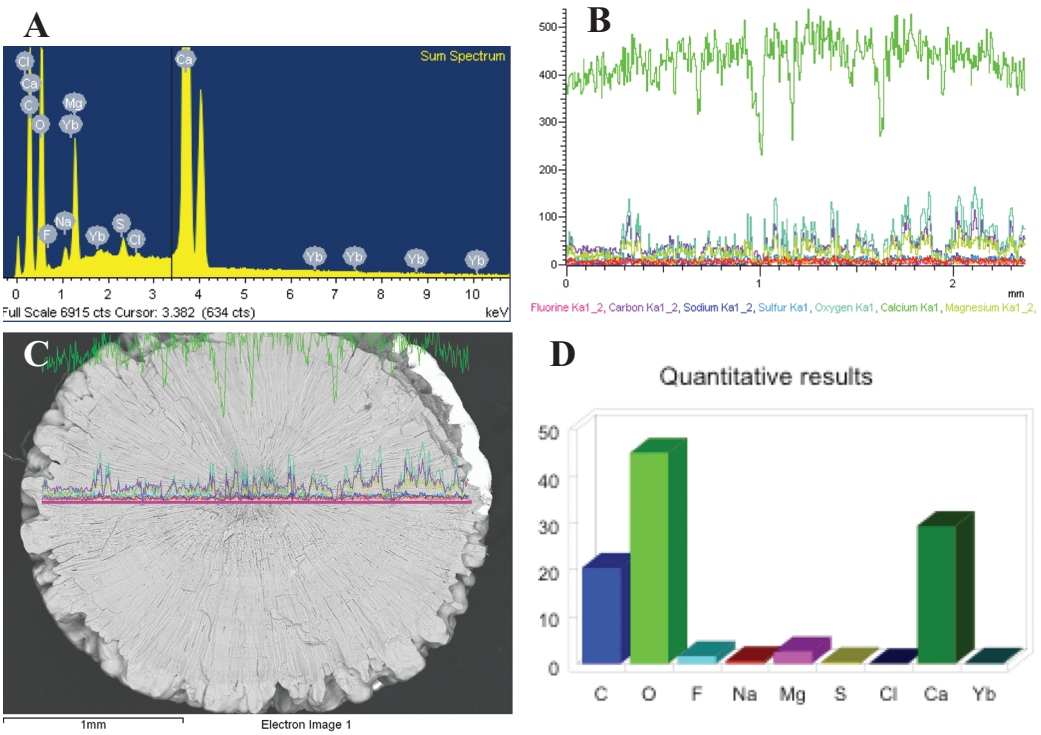

FIGURE 10. Energy dispersive spectrometer (EDS) linescan dataset. (A) EDS linescan site of interest BSE image in a cross-sectional view of a sea pen *Virgularia* sp. axial skeleton acquired by INCA Energy software using same region as Figure 9, horizontal linescan through the middle of the axis was applied for EDS analysis to examine the distribution of elements along the line. (B) Element linescan result displaying grouped linescans as colored: carbon (purple), oxygen (bright green), fluorine (pink), sodium (blue), magnesium (green), sulfur (teal), chlorine (red), calcium (light green), ytterbium (gold). (C) Sum spectrum of the linescan. Scale bar = 1 mm. (D) Bar chart of the quantitative results from the sum spectrum.

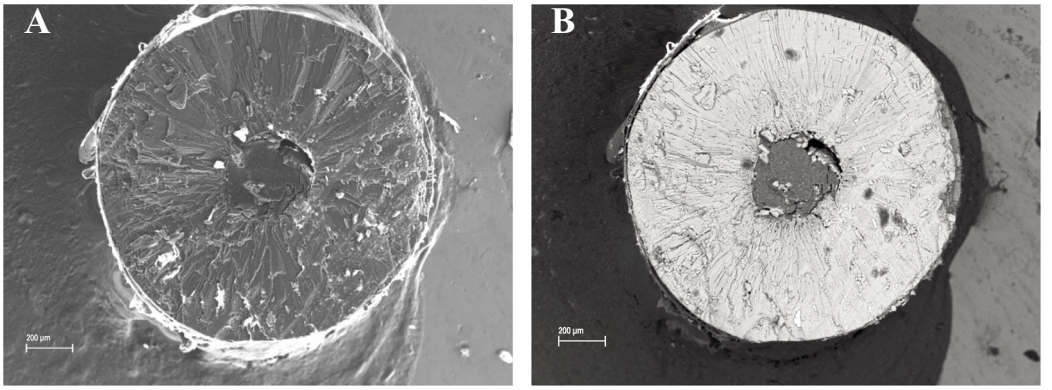

FIGURE 11. Scanning electron microscope (SEM) micrographs of a cross-sectional view of a sea pen *Stylatula* sp.axial skeleton. (A) Secondary electron (SE) image. The radiating patterns extending from the boundaries of the central core like that in *Virgularia* sp. are visible around the axis, and note that the central core is not prominent compared to that in the BSE image. Also visible are the charging effects on the scattered debris (possibly the contents coming from the hollow part of the central core) near the core and some places of the bottom axial surface. Scale bar = 200 µm. (B) Back-scattered electron (BSE) image. Atomic composition contrast is very strong on this image, where the central core is very distinctly shown in black/gray in comparison to the white peripheral axis regions. A few black dots with similar coloration as the central core are present on the axial surface near the top and the right of the image, likely the contents breaking from the core and attached on the axial surface. Scale bar = 200 µm.

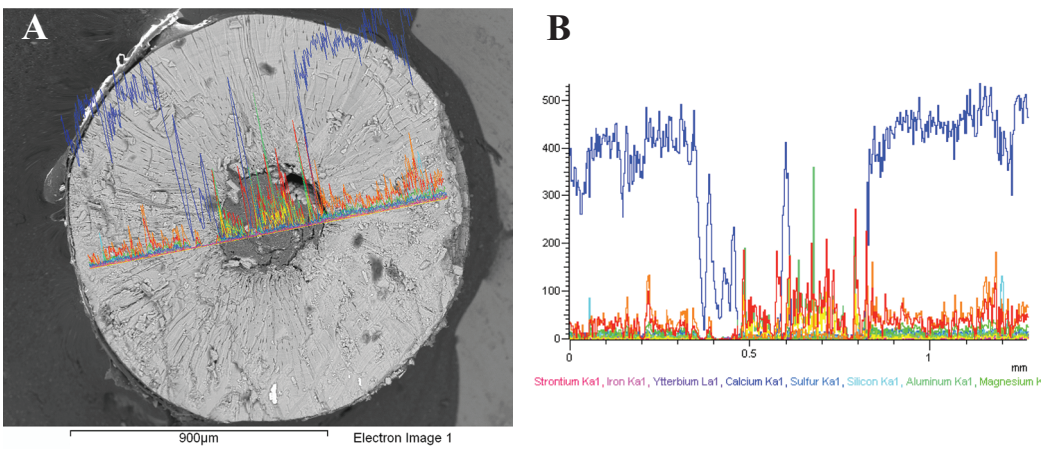

FIGURE 12. Energy dispersive spectrometer (EDS) linescan dataset. (A) EDS linescan site of interest BSE image in a cross-sectional view of a sea pen *Stylatula* sp. axial skeleton acquired by INCA Energy software using same region as Figure 11, horizontal linescan through the middle of the axis was applied for EDS analysis to examine the distribution of elements along the line. Scale bar = 900 µm. (B) Element linescan result displaying grouped linescans as colored: carbon (red), oxygen (orange), fluorine (yellow), sodium (green), magnesium (light green), aluminum (bright green), silicon (aqua), sulfur (light blue), calcium (blue), strontium (pink), ytterbium (purple), iron (hot pink).

***Stylatula* sp.**
Figures 11A–B, 12A–B, 13A–F.

From the element linescan graph Figure12B one can easily identify the dramatic drop of the calcium (in dark blue) weight percentage right on the range of the central core region, while other elements like carbon (in red), magnesium (in green), aluminum (in light green) and fluorine (in yellow) are increasing in value instead. Also noticeable are the void zones on both sides of the central core, which may probably be caused by the discontinuity of the surface on the boundaries between the core and the peripheral axis that ultimately resulted in the discontinuity of the X-ray detection as well. One single peak of calcium is shown in the central core region, which might be attributed to the broken pieces of debris from the more calcareous fringe of the core-axis intersection. The line patterns of most other elements like sodium (in dark green), silicon (in light blue), sulfur (in blue), strontium (in pink), ytterbium (in purple) and iron (in magenta) are relatively smooth compared to the big shifts of the line patterns of the elements mentioned above; thus, we know that those elements have more even overall distributions along the transect line.

Two area scans were performed between the two highly different atomic number contrast areas — the outer region of the axis and the central core — to determine the chemical compositions of the two distinct sites. From EDS results and the bar chart of spectrum 1, eleven elements were found as follows — three major elements: carbon (18.76 wt%), oxygen (40.09 wt%) and calcium (37.07 wt%); two minor elements: fluorine (1.47 wt%) and magnesium (1.48 wt%); and six trace elements: sodium (0.35 wt%), aluminum (0.08 wt%), iron (0.04 wt%), strontium (0.09 wt%) and REE ytterbium (0.22 wt%). The weight percentage of all elements can be seen in Table 6. This finding suggests that the outer region of the axis has a similar chemical distribution to most other species examined previously in having similar identified elements.

TABLE 6. EDS results of spectrum 1 for sea pen *Stylatula* sp. axial cross-section surface from Figure 13A. (All results are in weight%)

Element	C	O	F	Na	Mg	Al	S	Ca	Fe	Sr	Yb	Total
Spectrum 1 (Weight%)	18.76	40.09	1.47	0.35	11.48	0.08	0.35	37.07	0.04	0.1	0.22	100

Surprisingly, the EDS results from spectrum 2 showed dramatic changes in chemical composition of the central core; the most obvious change is the enormous drop in calcium weight percentage from 37.07 wt% to 0.32 wt%, making carbon a trace element, instead of as the always prominent major element; a large decrease in oxygen weight percentage is also observed, from 40.09 wt% to 8.46 wt%; while sulfur and iron weight percentage remain almost unchanged. Other changes include the addition of silicon and largely elevated amounts of carbon (from 18.76 wt% to 60.07 wt%), fluorine (from the previously 1.47 wt% to 24.14 wt%), and aluminum (from 0.08 wt% to 5.57 wt%), which make fluorine now a major element and aluminum now a minor element. The new discovery of barium is also surprising inasmuch as no other species examined here has been shown to contain barium. The overall element list for the identified twelve elements of spectrum 2 is shown in Table 7.

TABLE 7. EDS results of spectrum 2 for sea pen *Stylatula* sp. axial cross-section surface from Figure 13A. (All results are in weight%)

Element	C	O	F	Na	Mg	Al	Si	P	S	Ca	Fe	Ba	Total
Spectrum 2 (Weight%)	60.07	8.46	24.14	0.02	0.08	5.57	0.25	0.04	0.32	0.32	0.09	0.64	100

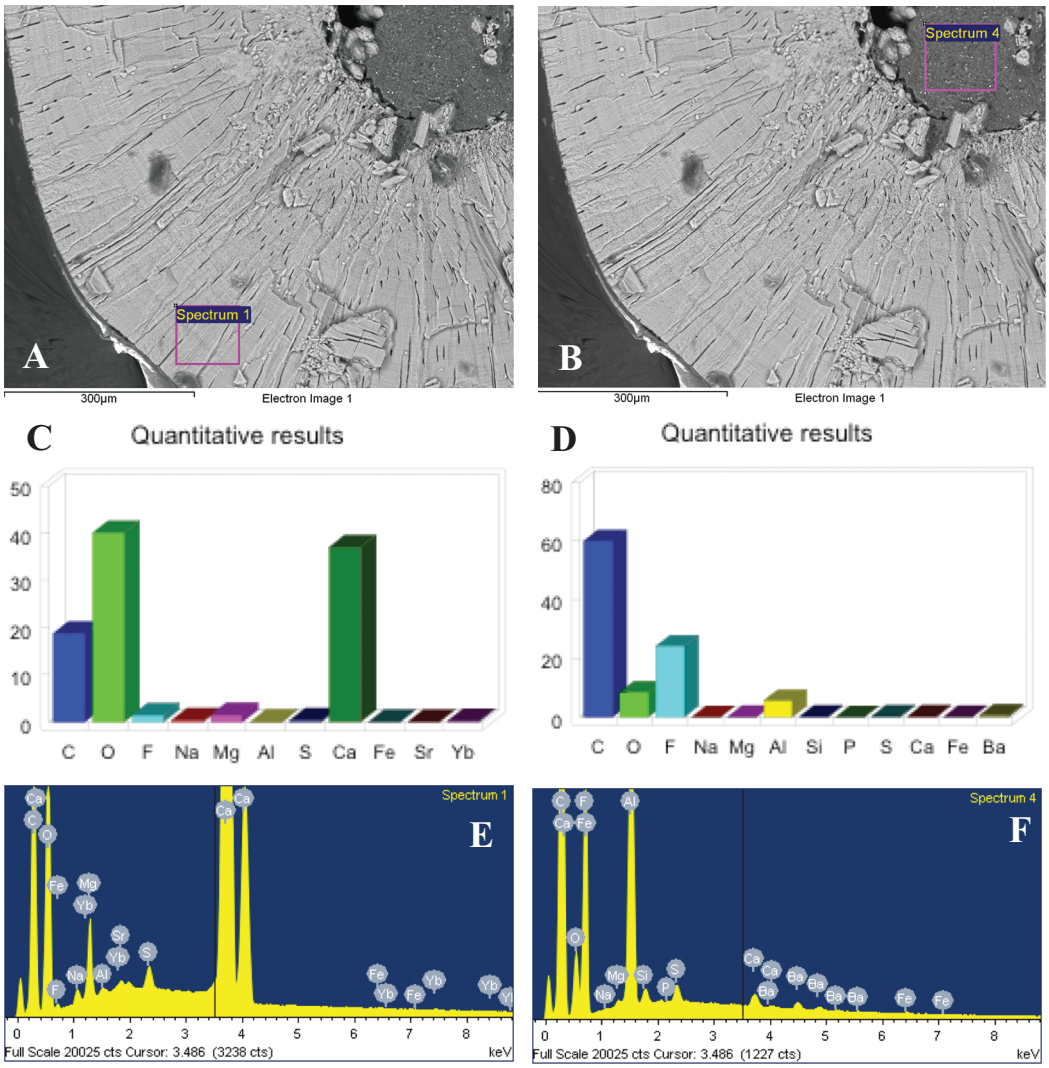

FIGURE 13. Energy dispersive spectrometer (EDS) area scan dataset. (A) and (B) EDS site of interest BSE image in a higher magnification cross-sectional view of the sea pen *Stylatula* sp. axial skeleton, acquired by INCA Energy software, partial area scans (spectrum 1 and 4) were applied for between site comparison purpose. Scale bar = 300 µm. (C) and (D) Bar charts of the quantitative results from spectrum 1 and spectrum 4. (E) and (F) EDS results for spectrum 1 and 4.

Among Taxa Comparison

The between-taxa comparison was made by selecting the shared elements by all species to be compared (Table 8), therefore trace elements like aluminum, silicon, phosphorous, chlorine, iron and bromine are not considered for comparison in this regard. Figure 14A shows the between-taxa elemental weight percentage comparison for the three gorgonians from three different families examined in this study: *Isis hippuris* (family Isididae), *Ellisella* sp. (family Ellisellidae) and *Plumigorgia hydroides* (family Plumigorgia). The trends of the three lines representing the three species are fairly similar and overlapping toward the end of chart where lies the higher atomic number elements; though some differences can be seen at the weight percentage value of carbon, oxygen, fluorine and magnesium.

TABLE 8. Summary of element distributions across taxa.

Elements shared by both gorgonians and sea pens:	C, O, F, Na, Mg, S, Ca, Yb
Elements shared by the three gorgonians:	C, O, F, Na, Mg, S, Ca, Sr, Yb
Elements shared by the four sea pens:	C, O, F, Na, Mg, S, Ca, Yb

Figure 14B shows the between-taxa elemental weight percentage comparison for the three sea pens from two different families examined in this study: *Cavernularia* sp. (family Veretillidae), *Virgularia* sp. (family Virgulariidae) and *Stylatula* sp. (family Virgulariidae). The trends of the lines representing *Cavernularia* sp. and *Virgularia* sp. are almost identical and differ only at the weight percentage value of the three major elements carbon, oxygen, and calcium. However, the line pattern of *Stylatula* sp. is significantly different from the two other species on all points of elements being compared, which is no doubt attribututable to the bizarre chemical composition of the central core inside the axial skeleton.

The line chart presented in Figure 15 shows the great similarities on the elemental weight percentage comparison of eight common elements among the three gorgonians: *Isis hippuris* (family Isididae), *Ellisella* sp. (family Ellisellidae) and *Plumigorgia hydroides* (family Plumigorgia) and two sea pens: *Cavernularia* sp. (family Veretillidae), *Virgularia* sp. (family Virgulariidae). Although the weight percentage difference are visible at some points, it is still considered as having identical trends across taxa, except *Stylatula* sp. (family Virgulariidae), which has a very different line pattern due to the peculiar chemical composition of its central axis core.

DISCUSSION

All EDS (Energy-dispersive X-ray spectroscopy) data shown here served as qualitative analyses only inasmuch as we were unable to achieve optimum quantitative accuracy inasmuch as the sample surfaces were unpolished (Oxford Instruments Plc. 2005). And, because of the unpolished samples, all EDS results were normalized by selecting the "All elements" processing option in "Quantitative Analysis Setup" section of the INCA software to force the analytical total to 100%. In addition, the carbon weight percent value is hard to define since the samples are all carbon coated. The reason to coat the samples with carbon is to prevent the M-family peaks of the metal-coating materials like platinum (Mα = 2.0485), iridium (Mα = 1.9779) and gold/palladium alloy (Au Mα = 2.1205, Pd Mα = 2.8387) from obscuring the identification and the analytical total of the K-family peaks of elements of interest, which may be present in the axial skeleton of the octocorals — such as silicon (Kα = 1.7398), phosphorus (Kα = 2.0134) and sulfur (Kα = 2.3075).

All six specimens examined herein had the presence of ytterbium, the rare earth element (REE); according to research conducted by Sholkovitz and Shen (1995), Fallon et al. (2002), Wyn-

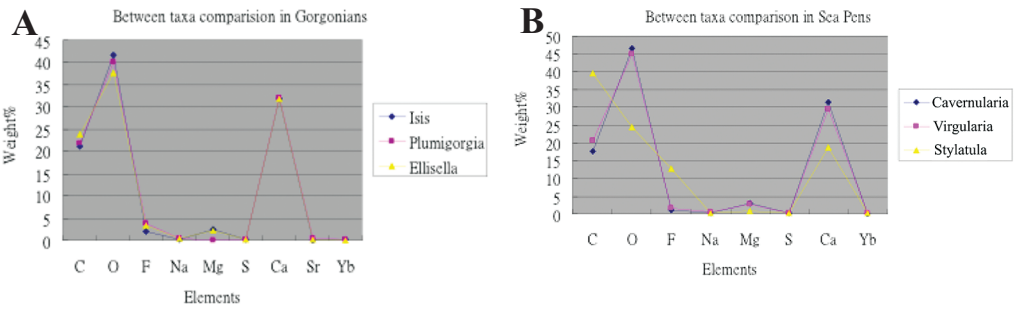

FIGURE 14. Line chart of the between-taxa elemental weight percentage comparison. (A) Between taxa comparison within the three gorgonians studied herein (*Isis hippuris, Plumigorgia hydroides* and *Ellisella* sp.). (B) Between taxa comparison within the sea pens studied herein (*Cavernularia* sp., *Virgularia* sp., and *Stylatula* sp.).

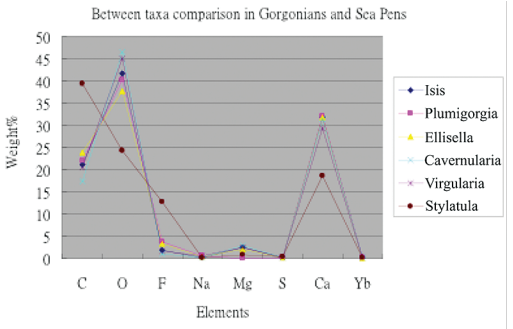

FIGURE 15. Line chart of the between-taxa elemental weight percentage comparison of both gorgonians and sea pens

dham et al. (2004) and Jupiter (2008), it is not rare to find REEs in coral skeleton lattices inasmuch as corals incorporate the REEs into the lattice by ionic substitution. The source of REEs and metals may come from the land via runoff events (Fallon et al. 2002), which may explain why various metals such as aluminum and iron can be found in some of the specimens, such as the *Stylatula* sp. collected right from the San Francisco Bay between Angel Island and Treasure Island, where there may be high degrees of impact due to the heavy populated locality.

The chemical composition across taxa between gorgonians and sea pens are for the most part similar and differ mostly by the trace elements that are present. As a result, the attempt to discern phylogenetic relationships depending on comparisons of chemical composition of axes among taxa is not sufficiently informative. However, it might seem promising to utilize the high-calcium content octocorals, such as the calcaxonian gorgonians and sea pens studied here, for environmental impact assessments in events like the *Deepwater Horizon* oil spill where impacts on deep-water octocorals were studied (White et al. 2012) or other anthropogenic influences such as mining and its impact on hard corals (Fallon et al. 2002). Both hard corals and octocorals as overall groups share similar extensive geographic and bathymetric ranges. Further investigation could compare the capability of recording ambient seawater elements in the skeletons of scleractinians with those in the axes of gorgonians and sea pens, preferably from the same transect site, to test the potential of using calcaxonian gorgonians and pennatulaceans for environmental impact studies.

Other than carbon, oxygen, and calcium, magnesium often shows a greater amount in some samples compared to the other minor elements. Folk (1974:45) states that sea water contains abundant magnesium ions and that any calcite cement that forms is rich in magnesium. An example would be cementing material that aids in the consolidation of octocoral axes.

Acknowledgements

This work was supported in part by NSF-MRI award CEM-0821619. We thank Dr. Andrew Ichimura for SEM and EDS instructions and everyone in BIOL 741 class. We also thank Forrest Horton for helping out with the epoxy mounting. We especially thank the Department of Invertebrate Zoology and Geology at the California Academy of Sciences for providing the octocoral specimens for this study. We thank the anonymous reviewers for critically reviewing the manuscript.

References

Anderson, C. A., and M. F. Hasler. 1966. Extension of electron microprobe techniques to biochemistry by the use of long wavelength X-rays. Pages 310–327 *in* R. Castaing, P. Deschamps, and J. Philibert, eds., *Proceedings of the 4th International Conference on X-ray Optics and Microanalysis*. Herman, Paris. France.

Bayer, F. M., and I. G. Macintyre. 2001. The mineral component of the axis and holdfast of some gorgonacean octocorals (Coelenterata: Anthozoa), with special reference to the family Gorgoniidae. *Proceedings of the Biological Society of Washington* 114:309–345.

Chen, J-Y. 2011. *Combined molecular and morphological evidence for phylogeny of pennatulacean and calcaxonian octocorals*. Master of Science Thesis in Marine Biology, San Francisco State University, San Francisco, California, USA. December 2011. 147 pp.

Fallon, S. J., J. C. White, and M. T. Andmcculloch. 2002. Porites corals as recorders of mining and environmental impacts: Misima Island, Papua New Guinea. *Geochimica et Cosmochimica Acta* 66:45–62.

Folk, R. L. 1974. The natural history of crystalline calcium carbonate: effect of magnesium content and salinity. *Journal of Sedimentary Petrology* 44(1):40–53.

Goldstein, J. I., D. E. Newbury, D. C. Joy, C. E. Lyman, P. Echlin, E. Lifshin, L. Sawyer, and J. R. Michael. 2003. *Scanning Electron Microscopy and X-ray Microanalysis, A Text for Biologists, Materials Scientists and Geologists.* Third edition. Springer, New York, New York, USA. 689 pp.

Grasshoff, M. 1999. The shallow-water gorgonians of New Caledonia and adjacent islands (Coelenterata: Octocorallia). *Senckenbergiana biologica* 78(1/2):1–121.

Grasshoff, M., and G. Bargibant. 2001. *Coral Reef Gorgonians of New-Caledonia*. Collection Faune et Flore Tropicale 38, Editions de IRD, Paris, France. 335 pp.

Jupiter, S. D. 2008. Coral rare earth element tracers of terrestrial exposure in nearshore corals of the Great Barrier Reef. Pages 102–106 *in* B. M. Riegl and R. E. Dodge, eds., *Proceedings.11th International Coral Reef Symposium,* Fort Lauderdale, Florida, USA.

Kanaya, K., and F. Okayama. 1972. Penetration and energy-loss theory of electrons in solid targets. *Journal of Physics* 5(1):43–58.

Kim, K., W. M. Goldberg, And G. T. Taylor. 1992. Architectural and mechanical properties of the Black Coral skeleton (Coelenterata: Antipatharia): a comparison of two species. *The Biological Bulletin* 182: 195–209.

Ledger, P. W., And S. Franc. 1978. Calcification of the collagenous axial skeleton of *Veretillum cynomorium* Pall (Cnidaria: Pennatulacea). *Cell and Tissue Research* 192:249–266.

Lewis, J. C., J. F. Barnowski, And G. J. Telesnicki. 1992. Characteristics of carbonates of gorgonian axes (Coelenterata, Octocorallia). *The Biological Bulletin* 183:278–296.

Macintyre, I. G., M. A. V. Logan, And H. C. W. Skinner. 2000. Possible vestige of early phosphatic biomineralization in gorgonian octocorals (Coelenterata). *Geology* 28(5):455–458.

Maia, L. F., R. A. Epifanio, And W. Fenical. 2000. New cytotoxic sterol glycosides from the octocoral *Carijoa* (*Telesto*) *riisei*. *Journal of Natural Products* 63:1427–30.

Oxford Instruments Plc. 2005. Inca Help Tutorials. Avaliable from: <*http://www.ebsd.com/incacrstal.htm*>

Shen, Y.-C., Y.-B. Cheng, Y.-C. Lin, J.-H. Guh, C.-M. Teng, And C.-L. Ko. 2004. New prostanoids with cytotoxic activity from Taiwanese octocoral *Clavularia viridis*. *Journal of Natural Products* 67:542–546.

SHOLKOVITZ, E., AND G. T. SHEN. 1995. The incorporation of rare earth elements in modern coral. *Geochimica et Cosmochimica Acta* 59:2749–2756.

WHITE, H. K., ET AL. 2012. Impact of the *Deepwater Horizon* oil spill on a deep-water coral community in the Gulf of Mexico. *Proceedings of the National Academy of Sciences* 109(50):20303–20308.

WILLIAMS, G. C. 1993. *Coral Reef Octocorals: An Illustrated Guide to the Soft Corals, Sea Fans, and Sea Pens Inhabiting the Coral Reefs of Northern Natal*. Durban Natural Science Museum, Durban, South Africa. 64 pp.

WYNDHAM, T., M. MCCULLOCH, S. FALLON, AND C. ALIBERT. 2004. High-resolution coral records of rare earth elements in coastal seawater: Biogeochemical cycling and a new environmental proxy. *Geochimica et Cosmochimica Acta* 68:2067–2080.